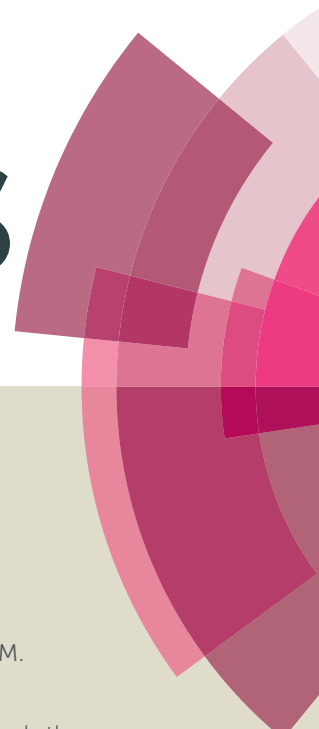


RSC Advances



This article can be cited before page numbers have been issued, to do this please use: S. CHILUKOTI, M. R. Gowravaram and R. Saraf, *RSC Adv.*, 2015, DOI: 10.1039/C5RA06864A.



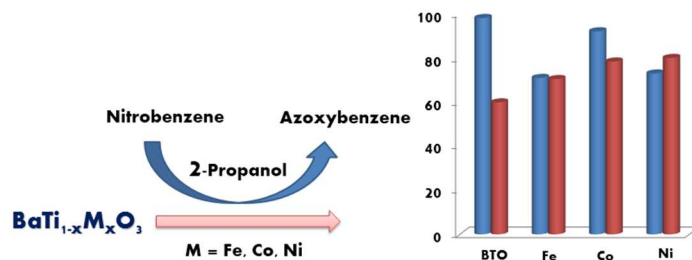
This is an *Accepted Manuscript*, which has been through the Royal Society of Chemistry peer review process and has been accepted for publication.

Accepted Manuscripts are published online shortly after acceptance, before technical editing, formatting and proof reading. Using this free service, authors can make their results available to the community, in citable form, before we publish the edited article. This *Accepted Manuscript* will be replaced by the edited, formatted and paginated article as soon as this is available.

You can find more information about *Accepted Manuscripts* in the [Information for Authors](#).

Please note that technical editing may introduce minor changes to the text and/or graphics, which may alter content. The journal's standard [Terms & Conditions](#) and the [Ethical guidelines](#) still apply. In no event shall the Royal Society of Chemistry be held responsible for any errors or omissions in this *Accepted Manuscript* or any consequences arising from the use of any information it contains.

Graphical extract



Highly active and selective Fe, Co and Ni doped BaTiO_3 catalysts for catalytic reduction of nitrobenzene to azoxybenzene was reported

Effect of nature of transition metal dopant in BaTiO₃ perovskite on catalytic reduction of nitrobenzene

Chilukoti Srilakshmi*^a, G. Mohan Rao^b and Rohit Saraf^a

^a*Solid State and Structural Chemistry Unit (SSCU), Indian Institute of Science (IISc), Bangalore, Karnataka, India, 560012*

^b*Department of Instrumentation and Applied Physics, Indian Institute of Science (IISc), Bangalore, Karnataka, India, 560012*

Email: ch.srilakshmi@sscu.iisc.ernet.in

Abstract

In the present study, we have synthesized Fe, Co and Ni doped BaTiO₃ by a wet chemical synthesis method using oxalic acid as chelating agent. The concentration of metal dopant varies from 0 to 5 mol. % in the catalysts. The physical and chemical properties of doped BaTiO₃ was studied using various analytical methods such as X-ray diffraction (XRD), Fourier transform infrared spectroscopy (FT-IR), BET surface area and Transmission electron microscopy (TEM). Acidic strength of the catalysts was measured using potentiometric titration method. Bulk BaTiO₃ crystalline phase exhibit tetragonal phase with *P4/mmm* space group. Structural transition from tetrahedral to cubic phase was observed for Fe, Co and Ni doped BaTiO₃ catalysts with increase in metal concentration from 1 to 5 mol.%. Particle size of the catalysts were calculated from TEM are in the range of 30-80 nm. All the catalysts were tested for the catalytic reduction of nitrobenzene to azoxybenzene. BaTiO₃ catalyst was found to be highly active and less selective compared to doped catalysts which are active and highly selective towards azoxybenzene. The increase in selectivity towards azoxybenzene is due to increase in acidic strength and reduction ability of the doped metal. It was also observed that nature of metal dopant and their content at B-site has an impact on the catalytic reduction of nitrobenzene. Co doped BaTiO₃ catalyst showed better activity with only 0.5 mol. % doping than Fe and Ni doped BaTiO₃ catalysts with maximum nitrobenzene conversion of 91% with 78% selectivity to azoxybenzene. An optimum Fe loading of 2.5 mol. % in BaTiO₃ is required to achieve 100% conversion with 93% selectivity whereas Ni with 5 mol.% showed conversion of 93% and a azoxybenzene selectivity of 84%.

Introduction

BaTiO₃ (BTO) is one of the most important ferroelectric material with a wide range of applications in nonlinear optics, multilayer ceramic capacitors (MLCs), actuators, transducers, ferroelectric random access memories (FRAM), micro-electro mechanical systems (MEMS), PTC thermistors, microwave devices, different type storage information devices, infrared sensors etc.¹⁻⁶ BTO has a general ABO₃ type structure where A and B are cations of different sizes with 6 fold coordinate B cation in the middle and the 12 fold coordinate A cation in the corner and the anion, commonly oxygen, in the center of the space. The phase of BTO at room temperature is tetragonal and it transforms to cubic above Curie temperature $T_c \sim 130^\circ\text{C}$. It also exists in orthorhombic phase at 0 °C and rhombohedral phases at below -90 °C and above 1460 °C it exists in hexagonal phase.⁷ It has been reported that the ferroelectric properties of BTO can be efficiently controlled by doping with different elements and the reported literature on the Fe, Co and Ni doped BTO catalyst are limited to studying electric and magnetic properties of these materials.⁸⁻¹¹ To the best of our knowledge there are only very few or no reports on the catalysis of these materials mainly for liquid phase organic transformations. Recently we have published Fe doped BaTiO₃ catalyst for the catalytic reduction of nitrobenzene.¹² In this context, present study is carried out to explore these materials for the catalytic reduction of nitrobenzene and study the effect of nature of dopant on the catalytic property. In continuation of our previous work we have explored doping of various metals such as Co and Ni including Fe with lower metal loading of 0.5 to 5 mol.% in BaTiO₃ in order to investigate the effect of metal dopant in B-site on the physico-chemical and catalytic properties of BaTiO₃ material.

The catalytic reduction of nitroarenes is an important reaction and the products such as aromatic amines or azoxy compounds are used in producing agrochemicals, pharmaceuticals,

dyes, pigments etc.¹³⁻¹⁵ and continuous efforts have been devoted to develop efficient production techniques. Since the conventional non-catalytic routes that use either the Fe/HCl system (Bechamp procedure) or metal sulfides inevitable generate large amount of wastes,¹⁵ and hence green and environmentally friendly selective reduction process is desired. Noble metal based such as Au, Pt, Pd¹⁶⁻¹⁹ are found to be highly effective catalysts for hydrogenation/reduction. However, the high price and scarcity of these precious metals are main drawbacks that hindered their large scale industrial application and these metals are sensitive to moisture and air when they are in complex forms.²⁰ As an alternative, there is a demand to use a number of cost effective metals hence in the present study we have explored Fe, Co and Ni doped BaTiO₃ catalysts for the selective reduction of nitrobenzene to azoxybenzene.

Experimental

Materials

All the metal nitrates and oxalic acid were purchased from Merck. Titanium isopropoxide was purchased from Sigma Aldrich. All chemicals are of analytical grade and used without further purification.

Synthesis of pure and metal doped BaTiO₃ (BTO) nanoparticles

The synthesis of BTO nanopowders by oxalate route²¹ was carried out starting with titanium isopropoxide and barium nitrate as metal oxide precursors, and oxalic acid as chelating agent, and 2-propanol as the solvent. These materials were mixed in a molar ratio Ti (OC₃H₇)₄ : Ba (NO₃)₂ : C₂H₂O₄·2H₂O = 1:1:2 in a mixture of 2-propanol and water. A homogeneous solution was obtained after stirring at 60 °C for 1h. Then the solution was evaporated to dryness at 100 °C. The oxalate precursors were then dried at 120 °C for overnight and calcined at 900 °C for 12

h for obtaining BaTiO₃ nanopowders. For metal substituted BaTiO₃ catalysts similar method was followed except the stoichiometric addition of dopant in the form of metal nitrate precursor to the above solution in the following ratio Ba(NO₃)₂ : 1-xTi(OC₃H₇)₄ : x M(NO₃)₂ : C₂ H₂O₄·2H₂O where x = 0.0 ≤ x ≤ 0.05 (where M = Fe, Co, Ni), respectively.

Catalyst characterization

The catalysts were characterized by x-ray diffraction recorded on a JEOL JDX-8030 x-ray diffractometer using CuK α radiation. The BET surface area of the catalysts was measured using a Model-Quantachrome Autosorb iQ₂ automated gas sorption analyzer. The catalysts were initially pretreated in N₂ at 300 °C for 6 h and the surface area of the catalysts was obtained by adsorbing N₂ at liquid nitrogen temperature, -196 °C.

The infrared absorption spectra were measured at room temperature, in the wave number range of 4000 to 400 cm⁻¹ by a computerized spectrometer type Perkin FTIR-300 using the KBr pellet technique. The particle size and morphology of the powders were studied using the transmission electron microscope (Model FEI Technai T20). Acidity of the solids was measured by means of potentiometric titration method. A known mass of solid suspended in acetonitrile was stirred for 3 h and then the suspension was titrated with a solution of 0.05N n-butylamine in acetonitrile, at a flow rate of 0.02 ml/min. The variation in electrode potential was measured with an instrument having a digital pH meter using saturated calomel electrode. The acidity measured by this method enables determination of total number of acidic sites and their strength. In order to interpret the results it is suggested that the initial electrode potential (E_i) be taken as the maximum acidic strength and the range where the plateau is reached (meq/g) can be considered as the total number of acid sites.²² The acidic strength of

the surface sites can be assigned as according to the following ranges.²³ Very strong site, $E_i > 100$ mV; strong site, $0 < E_i < 100$ mV; weak site $-100 < E_i < 0$ mV; very weak site, $E_i < -100$ mV.

Catalytic activity

Catalytic reduction with 2-propanol as hydrogen donor was carried out under continuous stirring in a two-necked 100 ml round bottom flask fitted with a reflux condenser. Analysis was done by withdrawing definite aliquots of the sample at regular intervals. In a typical run, 150 mg of the catalyst was dispersed in a solution containing 20 mmol of nitrobenzene, 20 mmol of KOH pellets and 20 ml of 2-propanol. The mixture was stirred and heated under reflux for 2–6 h in an oil bath. GCMS analysis of the product samples was carried out using Thermo Trace GC Ultra (GC), Thermo DSQ II (MS); with DB5 MS column of 30m L x 0.25mm ID x 0.25 μ m film thickness and with Electron Multiplier detector.

Results and discussion

Powder X-ray diffraction

Figure 1. shows the PXRD patterns of $\text{BaTi}_{1-x}\text{M}_x\text{O}_3$ ($\text{M} = \text{Fe}, \text{Co}, \text{Ni}; 0.0 \leq x \leq 0.05$) powders calcined at 900 °C for 12 h. From PXRD patterns, it can be clearly seen that the BaTiO_3 (BTO) exhibit tetragonal symmetry with space group $P4/mmm$. BaTiO_3 phase in the sample is confirmed by comparing the d values with the standard pattern JCPDS no. 075-0462. XRD patterns of the 0.5 mol. % metal doped BTO catalysts were matching with the tetragonal phase of BaTiO_3 whereas structural transition from tetragonal to cubic phase of BTO was observed with further increase in metal dopant concentration from 1 to 5 mol. % and matched with the corresponding standard pattern JCPDS no.074-1962 which indicates doping at B site and hereafter the doped catalysts were represented as BTO-M- with the number represents mol. % of

metal content. Traces of TiO_2 was found as impurity at 2θ of 28.46° and 29.62° in the catalysts.

The average crystallite size of the catalysts were calculated using Scherer formula:

$$D = \frac{0.9\lambda}{\beta \cos\theta}$$

where D is the average grain size, $\lambda=1.541 \text{ \AA}$ (X-ray wavelength), and β is the width of the diffraction peak at half maximum for the diffraction angle 2θ . The average crystallite size of the doped catalysts calculated from XRD (Table 2) was in the range of 30 – 50 nm whereas the size of the BTO sample was 81 nm.

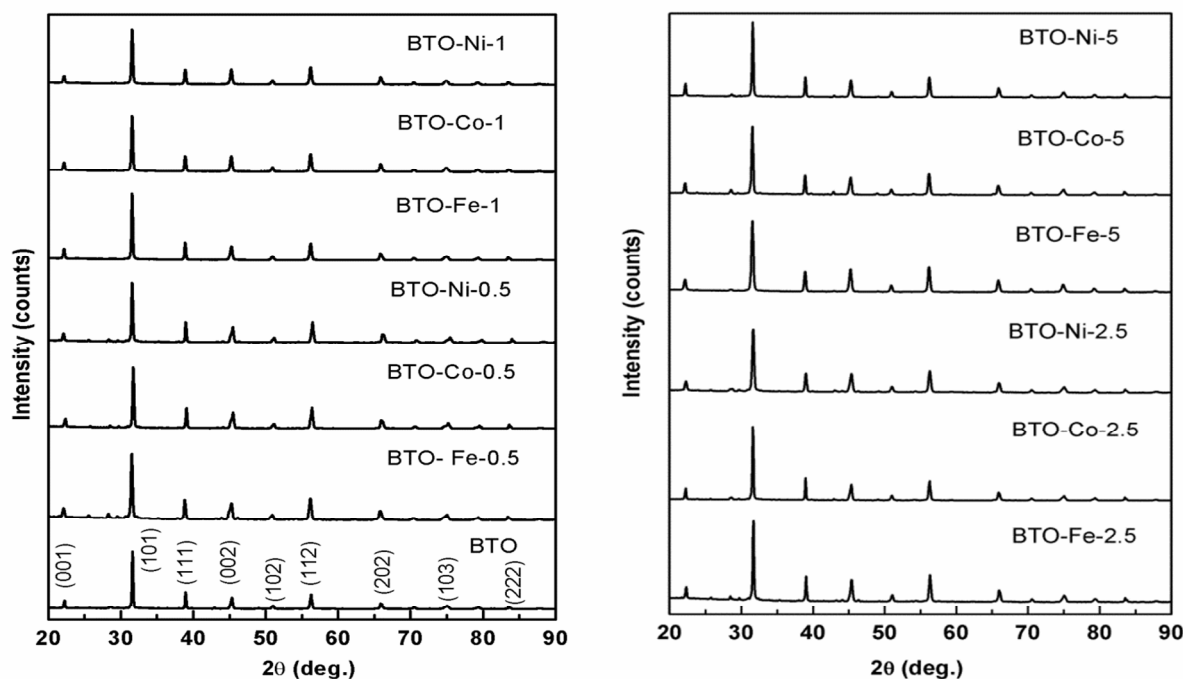


Figure 1. XRD spectra of BTO and various metals doped BTO catalysts

The cubic and tetragonal structures of BaTiO_3 were detected in the bulk and metal doped catalysts. In order to distinguish between two phases, the commonly used characteristic peak in the diffraction pattern, ranges between $2\theta = 40^\circ - 50^\circ$ region, where the single cubic (200) line

splits into two tetragonal peaks (200) and (002). For detailed structural analysis and to confirm doping XRD data was further analyzed by Reitveld refinement using FullProf suite programme and the refined structural parameters are given in Table 1. Figure. 2 show the experimental and calculated XRD pattern for tetragonal BTO and cubic BTO-Ni-1. The fitting between the experimental spectra and calculated values is relatively good based on the consideration of relatively lower R_p and R_{wp} ($< 10\%$) values. The unit cell parameters (crystal system, cell volume, space group and lattice parameters) are estimated by utilizing pseudo-voigt function. It was observed that the pure BaTiO_3 crystallized in the tetragonal structure with $P4mm$ space group. When the dopant metal (Fe, Co and Ni) concentration is 0.5 mol.%, all the diffraction peaks are consistent with the tetragonal phase but the cell volume increased as compared to pure BaTiO_3 . The phase transformation from tetragonal to cubic takes place, when the dopant metal concentration increased from 1 to 5 mol.%. The cell volume of cubic Fe, Co and Ni (1-5 mol.%) doped BaTiO_3 with space group $Pm-3m$ is higher than pure tetragonal BaTiO_3 . The increase in cell volume in the doped catalysts confirmed that the transition metal is being successfully incorporated into the crystal structure of BaTiO_3 .

Table 1. Refined structural parameters for BTO and various metal doped BTO catalysts.

| Sample | Space group | Lattice parameter (Å) | | Volume in (Å ³) |
|-------------|--------------|-----------------------|------------|-----------------------------|
| | | <i>a</i> | <i>c</i> | |
| BTO | <i>P4mm</i> | 3.9968(1) | 4.0280(1) | 64.345 (3) |
| BTO-Fe-0.5% | <i>P4mm</i> | 3.9903(3) | 4.0239 (3) | 64.352 (9) |
| BTO-Co-0.5% | <i>P4mm</i> | 4.0014(2) | 4.0265 (3) | 64.471 (7) |
| BTO-Ni-0.5% | <i>P4mm</i> | 4.0016(2) | 4.0253 (3) | 64.458 (7) |
| BTO-Fe-1% | <i>Pm-3m</i> | 4.0099(4) | 4.0099(4) | 64.481 (1) |
| BTO-Co-1% | <i>Pm-3m</i> | 4.0104(3) | 4.0104(3) | 64.501 (7) |
| BTO-Ni-1% | <i>Pm-3m</i> | 4.0117(1) | 4.0117(1) | 64.565 (3) |
| BTO-Fe-2.5% | <i>Pm-3m</i> | 4.0124(3) | 4.0124(3) | 64.596 (9) |
| BTO-Co-2.5% | <i>Pm-3m</i> | 4.0118(3) | 4.0118(3) | 64.568 (9) |
| BTO-Ni-2.5% | <i>Pm-3m</i> | 4.0129(2) | 4.0129(2) | 64.625 (5) |
| BTO-Fe-5% | <i>Pm-3m</i> | 4.0095(2) | 4.0095(2) | 64.459 (5) |
| BTO-Co-5% | <i>Pm-3m</i> | 4.0103(4) | 4.0103(4) | 64.498 (1) |
| BTO-Ni-5% | <i>Pm-3m</i> | 4.0100(3) | 4.0100(3) | 64.483 (8) |

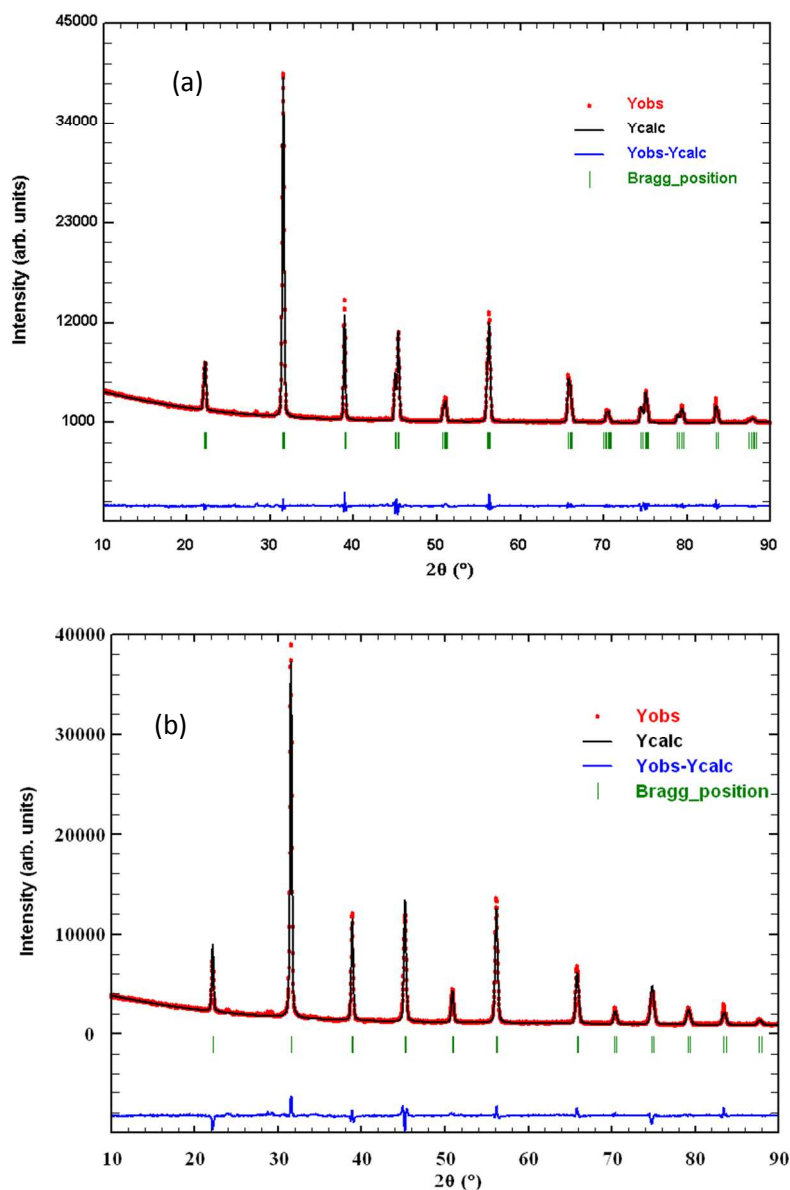


Figure 2: The observed, calculated and difference diffraction profiles from Rietveld refinement of (a) tetragonal BTO (b) cubic BTO phase in BTO-Ni-1%.

Fourier Transform Infrared Spectroscopy

The FT-IR spectra of the catalysts measured are shown in Figure 3. The IR spectrum of the catalysts consists mainly of two regions: the first region shows bands (not shown here) at circa

3428-3436 which was due to the OH stretching vibration (ν) of surface hydroxyls of the barium titanate catalyst. The TG results (Figure S2, ESI) clearly suggest that there is no surface H_2O is present below 150°C . However the total weight loss of 0.6 % was observed below 900°C . Hence the same has been ascribed to surface hydroxyls in the FT-IR. The second region, in the range between $392\text{-}600\text{cm}^{-1}$, represents the characteristic infrared absorptions of the Ti-O vibrations. The band situated around $\sim 539\text{ cm}^{-1}$ is due to TiO_6 stretching vibration connected to the barium. The additional peaks at 857 cm^{-1} in the may be due to metal-oxygen band stretching. Finally, the peak at 396 cm^{-1} can be attributed to normal TiO_2 bending vibrations. Additional peaks corresponding to Fe-O, Co-O and Ni-O were not observed in the spectra of the metal doped BTO catalysts.

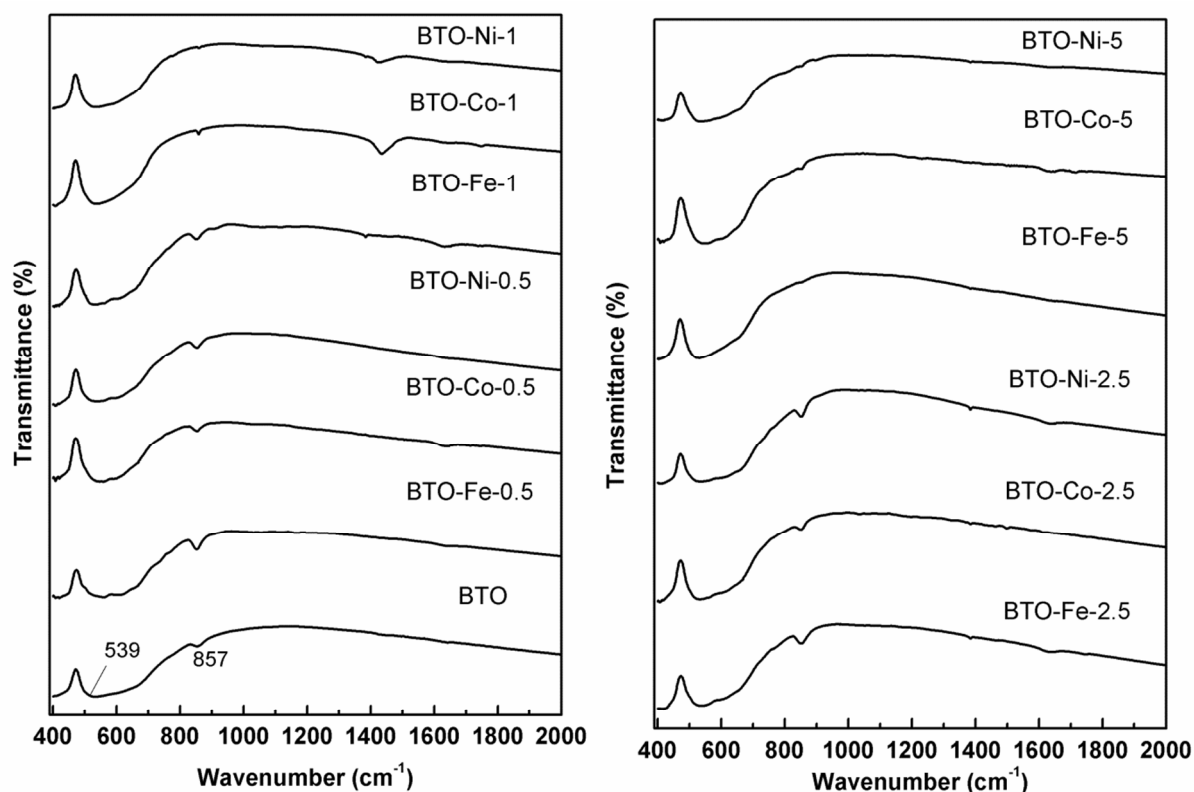


Figure 3. FTIR spectra of BTO and various metals doped BTO catalysts

Transmission electron microscopy

Figure 4. shows the transmission electron micrographs of the represent catalysts. Average grain size in the catalysts are in the range of 15-80 nm. Shape of the particles is spherical as well as cubic and is highly agglomerated. Grain size of the Co doped BTO catalysts (15-20 nm) was less compared to Fe and Ni as evident from Figure 4b and 4e. The decrease of grain size for Co-doped BTO catalysts could be due to suppression of oxygen vacancies due to charge compensation mechanism which results in slower oxygen ion motion and consequently lower grain growth rate. The same has been reported earlier for various metal doped in BiFeO_3 .^{24, 25}

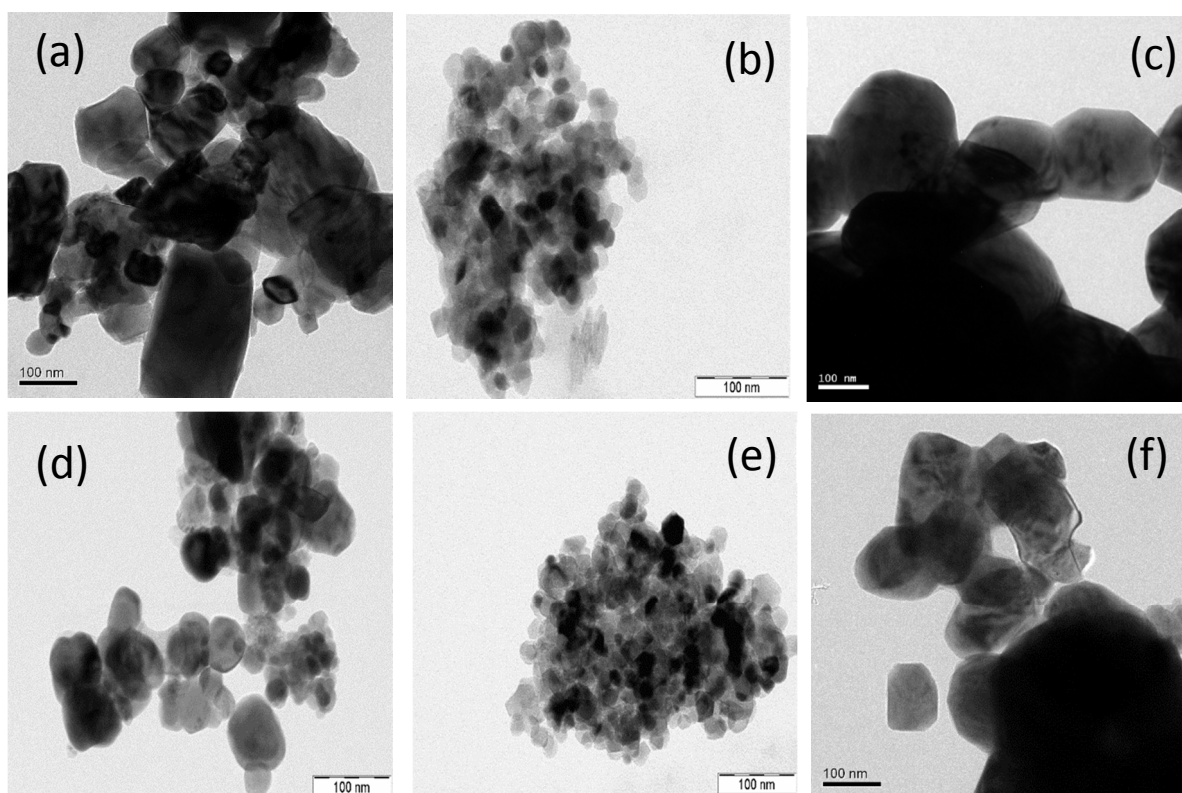


Figure 4. TEM images of the various doped BTO catalysts (a) BTO-Fe-1(b) BTO-Co-1(c) BTO-Ni-1(d) BTO-Fe- 5(e) BTO- Co-5(f) BTO-Ni-5

BET surface area and Acidic strength of catalysts

BET surface areas measured by N₂ physisorption and acidic strength of the catalysts are given in Table 2. Surface area of BTO was found to be 1.8 m²/g. The metal doped BaTiO₃ catalysts showed slight increase in the surface area measured by BET method. As the metal content increased in the BaTiO₃ the surface area also increased. This clearly suggests that the doped metal is providing additional surface to the BaTiO₃.

Table 2. Physico-chemical properties of various metals doped BTO catalysts

| Sample name | Surface area (m ² /g) | Crystallite size (nm) by XRD | Acidic strength, E (mV) |
|-------------|----------------------------------|------------------------------|-------------------------|
| BTO | 1.8 | 81.01 | 175 |
| BTO-Fe-0.5% | 2.0 | 34.57 | 193 |
| BTO-Co-0.5% | 10 | 30.86 | 221 |
| BTO-Ni-0.5% | 12 | 51.39 | 204 |
| BTO-Fe-1% | 3.8 | 34.06 | 203 |
| BTO-Co-1% | 13 | 37.32 | 191 |
| BTO-Ni-1% | 14 | 31.99 | 219 |
| BTO-Fe-2.5% | 4.2 | 39.22 | 196 |
| BTO-Co-2.5% | 15.5 | 37.62 | 218 |
| BTO-Ni-2.5% | 16.6 | 35.54 | 257 |
| BTO-Fe-5% | 5.8 | 49.94 | 194 |
| BTO-Co-5% | 18 | 32.35 | 200 |
| BTO-Ni-5% | 24 | 38.59 | 192 |

Acidic strength values, expressed as E (mV) are given in Table 2. It was observed from the table that strong or very strong acidic sites were present in all the catalysts since E_i values of all the catalysts were greater than 100 mV and it was observed that acidic strength of the doped catalysts was higher than that of pure BTO catalyst. This clearly indicates that doping enhanced the acidic strength of the catalysts.

Catalytic reduction of nitrobenzene to azoxybenzene

Blank reaction without catalyst has been carried out and no conversion of nitrobenzene has been observed under similar reaction conditions.

Activity of Fe doped BTO catalysts

It was observed from the activity profiles of various catalysts (Figures 5 and 6) that pure BTO catalyst was found to be more active and less selective with 98% conversion and 60% selectivity towards azoxybenzene. To increase the selectivity of BTO catalyst it has been doped with transition metals such as Fe, Co, Ni with varying metal loading in between 0.5 to 5 mol.%. It was observed that the selectivity was greatly improved with the compromise in nitrobenzene conversion. The results showed that with increase in Fe content (0 to 2.5%) in the BTO catalyst the conversion has been increased and reached to 100% over BTO-Fe- 2.5 and it remained constant with further increase in Fe content to 5%. Whereas the selectivity to azoxybenzene increased with increase in Fe content in BTO catalyst and showed a maximum selectivity of 93 % on BTO-Fe- 2.5 and it slightly decreased to 82 % on BTO-Fe- 5 while conversion remained constant. The decrease in selectivity on BTO-Fe-5% was due to formation of side products such as aniline and azobenzene respectively.

Activity of Co doped BTO catalysts

It was observed that Co doped (Figures 5 and 6) BTO catalysts showed high nitrobenzene conversion of 91 to 92% on BTO-Co- 0.5 and 1%. With further rise in Co loading (BTO-Co-2.5 and 5 %) the conversion has been reduced to 72% on Co 2.5 % and remained constant with further increase in Co content. Maximum selectivity of 78-80% was obtained on all the catalysts irrespective of the increase in Co content. The results reveal that high conversion for lower Co

content (BTO-Co- 0.5%) compared to Fe and Ni doped BTO catalysts where the higher conversion observed at higher metal content could be due to less particle size of 20 nm as observed from TEM and XRD crystallite size 30.86 nm (shown in Table 2) and the selectivity to azoxybenzene remained constant with increase in Co content in the catalysts it reveals that selectivity is independent of Co amount at higher loadings in the catalysts.

Activity of Ni doped BTO catalysts

It was observed from activity profiles (Figures 5 and 6) of Ni doped BTO catalysts that conversion increased with increase in Ni content and showed a conversion of 88% over BTO-Ni-1% thereafter there is a sudden drop in conversion to 56.8% was observed on BTO-Ni-2.5% and it increased with further rise in Ni content of BTO-Ni- 5% and achieved a maximum conversion of 93% and selectivity of 84% towards azoxybenzene.

It was concluded that nature of metal dopant and its percent loading at B-site has an impact on the catalytic reduction of nitrobenzene. And it was observed that Co required a relatively lower amount of 0.5 % in BTO catalyst in order to achieve good conversion and selectivity compared to Fe and Ni doped catalysts. Fe doped catalysts showed maximum conversion and selectivity at an optimum loading of Fe-2.5%. Whereas in order to achieve better conversion and selectivity the percentage of Ni required is 5%.

Correlation between acidic strength and yield of azoxybenzene

The bulk BaTiO₃ has showed the conversion of 98% and azoxybenzene selectivity of 60 %. By doping the metals Fe, Co and Ni into BaTiO₃ the selectivity showed considerable increase. There is no direct correlation between conversion and acidic strength or number of acid sites was observed (Figure S3, ESI). This is due to the fact that the metals are facilitating the reduction of

nitrobenzene and thus there was no direct relationship with conversion is observed. However we have found a good correlation between acidic strength of catalysts and yield of azoxybenzene was observed and the same has been shown in Figure 7. It was observed that with the increase in acidic strength of the catalyst the azoxybenzene yield increased initially and obtained a maximum yield of 93% at acidic strength of 196 mV on BTO-Fe-2.5% and further increase in acidic strength leads to decrease in yield of azoxybenzene this was due to formation of side products.

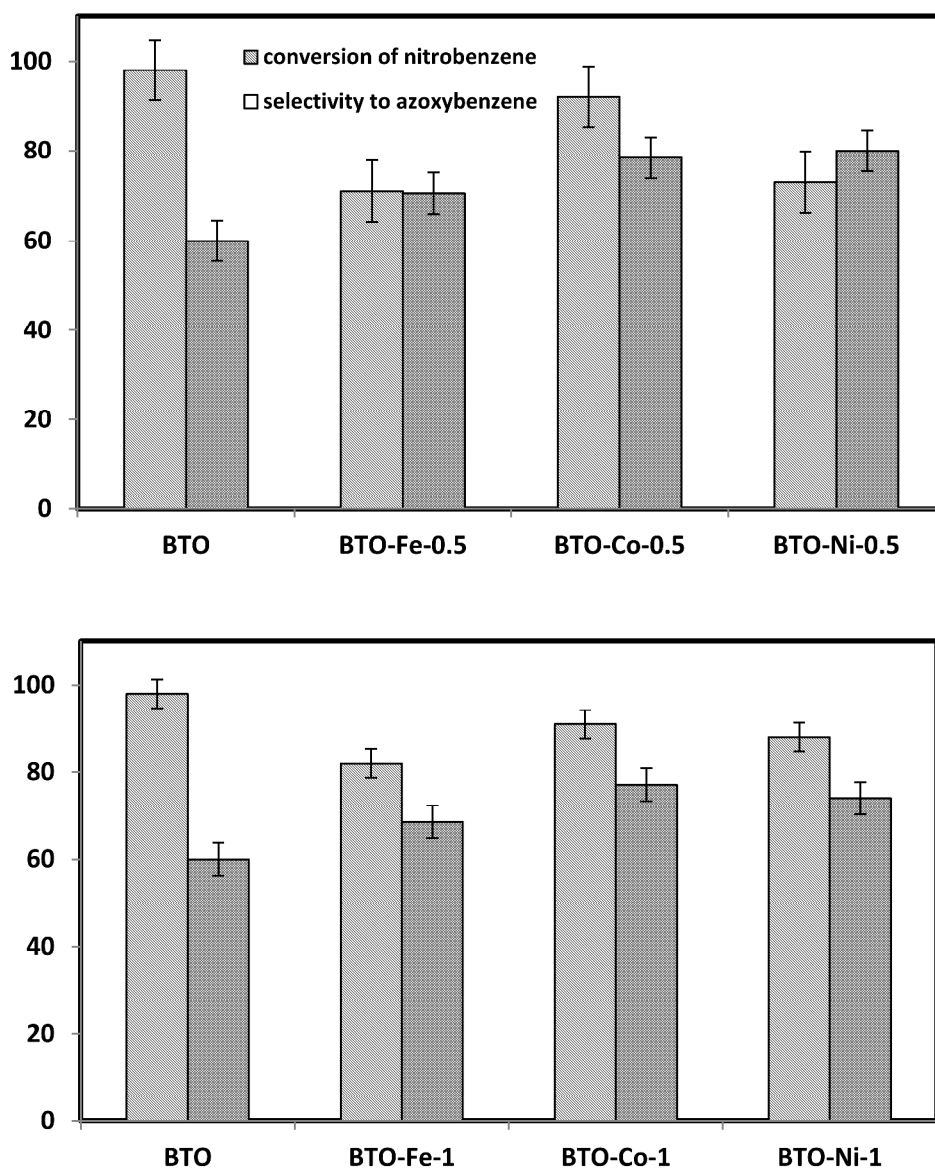


Figure 5. Activity profiles of various BTO catalysts for catalytic reduction of nitrobenzene (with metal loading of 0.5 and 1%)

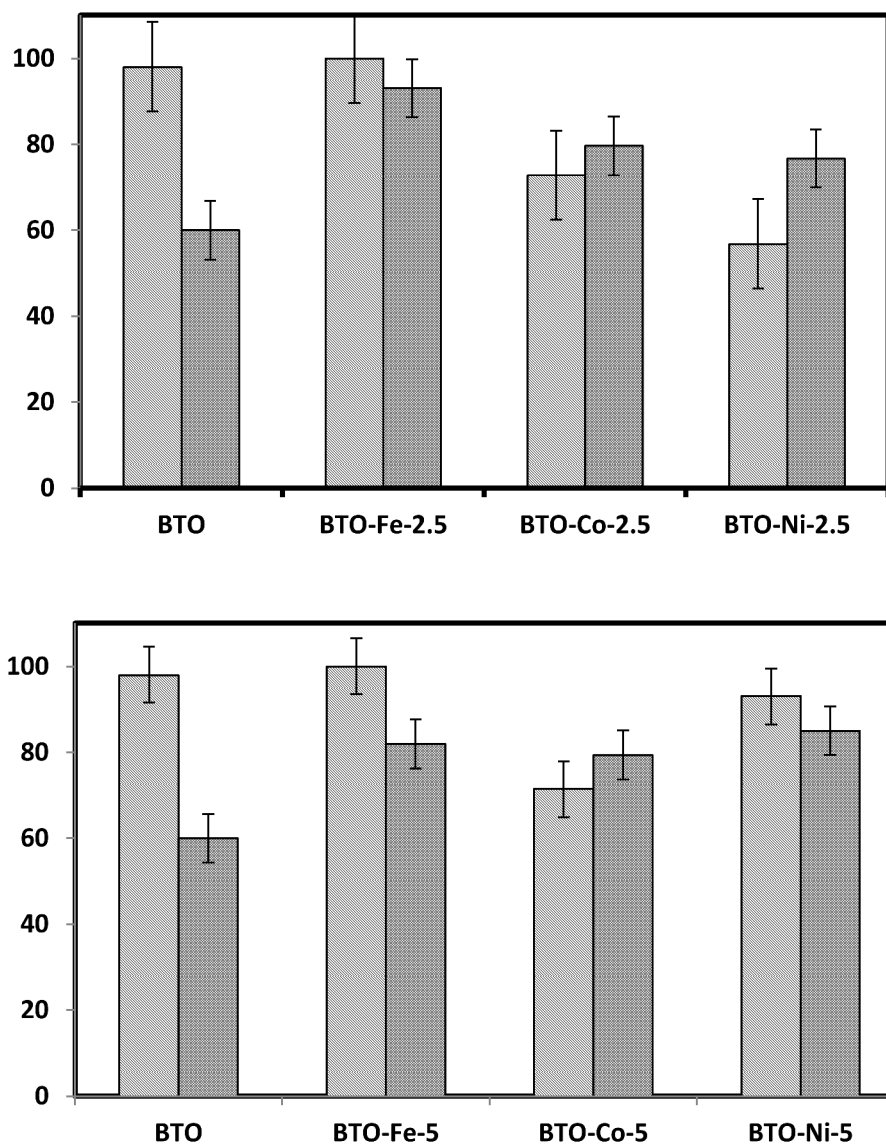


Figure 6. Activity profiles of various BTO catalysts for catalytic reduction of nitrobenzene (with metal loading of 2.5 and 5%)

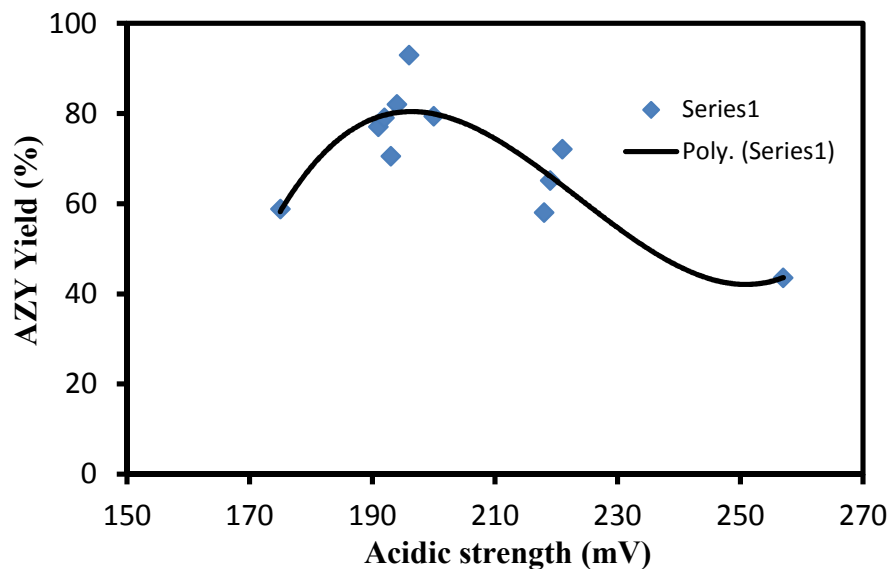


Figure 7: Correlation between Acidic strength and Yield of Azoxybenzene for BTO and metal doped BTO catalysts.

The most active catalyst i.e. BTO-Fe-2.5 was tested for the reusability (Table 3) and it was found that it could be reused without affecting the activity till at least three cycles.

Table 3: Recyclability of BTO-Fe-2.5 % catalyst for the catalytic reduction of nitrobenzene

| Sr. No | Cycle | Conversion | Selectivity to Azoxybenzene (%) |
|--------|-------|------------|---------------------------------|
| 1 | 0 | 100 | 93 |
| 2 | 1 | 100 | 91 |
| 3 | 2 | 100 | 92 |
| 4 | 3 | 100 | 90 |
| 5 | 4 | 83 | 75 |

Proposed mechanism

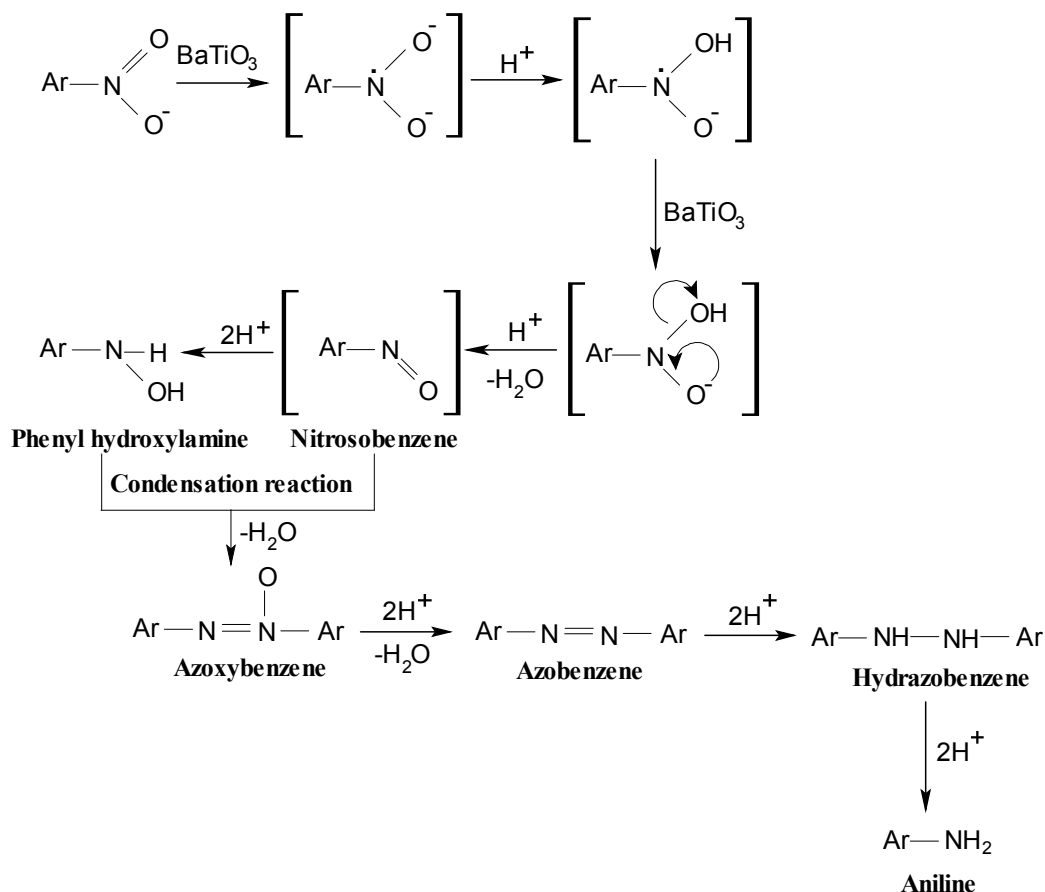


Figure 8: Proposed mechanism for catalytic reduction of nitrobenzene over BaTiO₃

A reaction mechanism was proposed for catalytic reduction of nitrobenzene in the presence of BaTiO₃ catalyst and 2-propanol as proton donor was shown in Figure 8. Reduction of nitrobenzene to azoxybenzene was due to electron transfer, followed by proton transfer and elimination of water molecule generates nitroso benzene intermediate which undergoes further two rounds of electron transfer and protonation to form phenyl hydroxylamine. Further condensation reaction between nitrosobenzene and phenyl hydroxylamine can lead to azoxybenzene which on further protonation and catalytic cleavage leads to azobenzene and aniline products.

Conclusions

In the present study, various transition metals such as Fe, Co, and Ni doped BaTiO₃ has been synthesized and the effect of metal dopant on the catalytic reduction of nitrobenzene was tested. Pure BaTiO₃ exists as tetragonal phase with *P4/mmm* space group. Structural transition from tetrahedral to cubic phase was observed in Fe, Co and Ni doped BaTiO₃ catalysts with metal content from 1 to 5 mol.%. The particle size of the catalysts calculated from TEM is in the range of 15 - 80nm. BaTiO₃ was found to be highly active and less selective for catalytic reduction of nitrobenzene compared to doped catalysts which are highly active and highly selective towards azoxybenzene. The results showed that the nature of metal dopant and their loading at B-site has an impact on the catalytic reduction of nitrobenzene. Based on the activity results, it is concluded that Co doped BaTiO₃ showed good conversion and selectivity at relatively lower Co content of 0.5 % compared to Fe and Ni doped catalysts with maximum 91% nitrobenzene conversion and 80% azoxybenzene selectivity. Fe doped BaTiO₃ catalyst required an optimum loading of 2.5% to achieve a maximum 100% conversion with 93% azoxybenzene selectivity. Whereas Ni dopant required a loading of 5 % to obtain maximum conversion of 93% with 85% selectivity towards azoxybenzene. Acidity measurements revealed that all the BaTiO₃ catalysts contain very strong acidic sites and acidic strength of the doped catalysts was higher than that of pure BTO catalyst. This clearly indicates that doping enhanced the acidic strength of the catalysts. A good correlation between acidic strength and yield of azoxybenzene was obtained. The catalytic results obtained in the present study indicate that transition metal doped BaTiO₃ material would be an interesting nanomaterial to explore for the catalytic reduction/ hydrogenation of various organic compounds.

Acknowledgements

This work was financially supported by Department of science and technology (DST) India through INSPIRE project. We would like to thank Mass Spectrometry Facility, Division of Biological Sciences, Indian Institute of Science for GC-MS analysis.

References

1. W. D. Maison, W. D. R. Kleeberg, R. B. Heimann, and S. Phanichphant, *J. Eur. Chem. Soc.*, 2003, **23**, 127.
2. J. S. Obhi and A. Patel, *Integr. Ferroelectric*, 1994, **5**, 155.
3. J. F. Scott, D. Galt, J. C. Price, J. A. Beall, R. H. Ono, C. A. Paz de Araujo and L. D. McMillan, *Integr. Ferroelectric*, 1995, **6**, 189.
4. M. A. Mohiddon, P. Goel, K. L. Yadav, M. Kumar and P. K. Yadav, *Indian J. Eng. Mater. sci.*, 2007, **14**, 64.
5. S. Mathews, R. Ramesh, T. Venkatesan, and J. Benedetto, *Science*, 1997, **276**, 238.
6. B. H. Park, B. S. Kang, S. D. Bu, T. W. Noh, J. Lee and W. Jo, *Nature*, 1999, **401**, 682.
7. G. M. Keith, M. J. Rampling, K. Sarma, N. Mc. Alford, and D. C. Sinclair, *J. Eur. Ceram. Soc.*, 2004, **24**, 1721.
8. F. Jona and G. Shirane, *Ferroelectric Crystal* (Dover, Publication, New York) 1993.
9. P. Goel and K. L. Yadav, *J. Mater. Sci.*, 2007, **42**, 3928.
10. P. Goel, K. L. Yadav and A. R. James, *J. Phys.D: Appl Phys.*, 2004, **37**, 3174
11. M. A. Mohiddon and K. L. Yadav, *Sol-Gel Sci. Technol.*, 2009, **49**, 88.
12. Ch. Srilakshmi, H. Vijay Kumar, K. Praveena, C. Shivakumara and M. Muralidhar Nayak, *RSC Adv.*, 2014, **4**, 18881.
13. R. S. Downing, P. J. Kunkeler and H. Van Bekkum, *Catal. Today*, 1997, **37**, 121.

14. G. Wegener, M. Brandt, L. Duda, J. Hoffman, B. Kleszczewski, D. Koch, R. J. Kumpf, H. Orzesek, H. G. Pirkl, C. Six, C. Steinlein and M. Weisbeck, *Appl. Catal. A*, 2001, **221**, 303.
15. K. Nomura, *J. Mol. Catal. A*, 1998, **130**, 1
16. A. Corma and P. Serna, *Science*, 2006, **313**, 332
17. E. A. Gelder, S.D. Jackson and C. M. Lok, *Catal. Lett.*, 2002, **84**, 205.
18. J. L. Zhang, Y. Wang, H. Ji, Y. G. Wei, N. Z. Wu, B. J. Zuo and Q. L. Wang, *J. Catal.*, 2005, **229**, 114.
19. F. Ragaini and S. Cenini, *J. Mol. Catal. A*, 1996, **105**, 145
20. R. V. Jagadeesh, G. Weinhofer, F. A. Westerhaus, A. E. Surkus, M. M. Pohl, H. Junge, K. Junge and M. Beller, *Chem. Commun.*, 2011, **47**, 10972.
21. A. Ianculescu, D. Berger, C. Matei, P. Budrugaec, L. Mitoseriu and E. Vasile, *J. Electroceram.*, 2010, **24**, 46.
22. P. Villabrille, P. Vazquez, M. Blanco and C. Caceres, *J. Colloid and Interface*, 2002, **251**, 151.
23. R. Cid and G. Pecchi. *Appl. Catal.*, 1985, **14**, 15.
24. M. Kumar and K. L. Yadav, *Appl. Phys. Lett.*, 2007, **91**, 242901.
25. R. Dahiya, A. Agarwal, S. Sanghi, A. Hooda and P. Godara, *J. Magn. Mater.*, 2015, **385**, 175